Indian Journal of Pure & Applied Physics
Vol. 54, August 2016, pp. 517-534

Hall effects on unsteady MHD natural convective flow past an impulsively moving plate with ramped temperature and concentration

S Das[a]*, R N Jana[b] & S K Ghosh[c]

[a]Department of Mathematics, University of Gour Banga, Malda 732 103, India

[b]Department of Applied Mathematics, Vidyasagar University, Midnapore 721 102, India

[c]Department of Mathematics, Narajole Raj College, Narajole, Midnapore 721 211, India

Received 8 November 2013; revised 31 December 2013; accepted 25 January 2014

This paper deals with the study of an unsteady magnetohydrodynamic natural convective flow of a viscous incompressible electrically conducting fluid past an impulsively moving infinite vertical plate with ramped temperature and mass concentration taken into account the Hall effects. A uniform magnetic field is applied transversely to the direction of the flow. The flow consideration is subjected to small magnetic Reynolds number. Induced magnetic field is absent. The Rosseland approximation is used to describe the radiative heat flux in the energy equation. Analytical solution of the governing equations has been obtained by employing the Laplace transform technique. The influences of the pertinent parameters on the velocity field, temperature distribution, mass concentration in fluid, shear stress and rate of heat and mass transfer are discussed with the help of graphs. Hall current is found to elevate the fluid velocity components. It is observed that significant difference can be observed between the velocity profiles due to ramped and isothermal boundary conditions.

Keywords: MHD natural convection, Vertical plate, Thermal radiation, Ramped temperature, Concentration

1 Introduction

In many engineering applications, especially in heat exchangers, heat transfer improvement is an important issue. The plate heat exchangers are the most important in most of the industries such as food processing, drug and chemical industries. Boundary layer theory is an important aspect in the study of a continuously stretching surface into aquiescent fluid, a flows cenario that has garnered much attention over several decades. Some of applications that involve this scenario include hot rolling, paper production, metal spinning, drawing plastic films, glass blowing, continuous casting of metals, and spinning of fibers. Natural or free convection is a physical process of heat and mass transfer involving fluids which originates when the temperature as well as species concentration change cause density variations inducing buoyancy forces to act on the fluid. Such flows exist abundantly in nature and due to its applications in engineering and geophysical environments, these have been studied extensively in practice. Welty *et al.*[1] defines mass transfer as the transport of one constituent from a region of higher concentration to that of a lower concentration. Mass transfer is the basis for many biological and chemical processes. Biological processes include the oxygenation of blood and the transport of ions across membranes within the kidney. Mass transfer also occurs in many other processes such as absorption, drying, precipitation, membrane filtration and distillation. Another process of heat transfer is radiation through electromagnetic waves. Many engineering processes such as fossil fuel combustion energy processes, solar power technology, astrophysical flows and space vehicle re-entry occur at high temperature, so radiative heat transfer plays very important role. Also thermal radiation on flow and heat transfer processes is of major interest in the design of many advanced energy conversion systems operating at high temperature. Thermal radiation effects become important when the difference between the surface and the ambient temperature is large. Radiative convective flows are encountered in several industrial and environmental processes. The study of radiation interaction with convection for heat and mass transfer in fluids is quite significant. The heating of rooms inside buildings using radiators is an example of application of heat transfer by free convection. Sometimes along with the free convection currents caused by difference in temperature of the

*Corresponding author (E-mail: jana261171@yahoo.co.in)

flow is also affected by the differences in concentration or material constitution. There are many situations where convection heat transfer phenomena are accompanied by mass transfer also. When mass transfer takes place in a fluid at rest, the mass is transferred purely by molecular diffusion resulting from concentration gradients. For low concentration of the mass in the fluid and low mass transfer rates, the convective heat and mass transfer processes are similar in nature. A number of investigations have already been carried out with combined heat and mass transfer under the assumption of different physical situations. The illustrative examples of mass transfer can be found in the book of Cussler[2]. Combined heat and mass transfer flow past a surface analyzed by Chaudhary *et al.*[3], Muthucumaraswamy *et al.*[4-6] and Rajput *et al.*[7] with different physical conditions. Juncu[8] pioneered unsteady heat and mass transfer flow past a surface by numerical method. Das *et al.*[9] considered the effects of first order chemical reaction on the flow past an impulsively started infinite vertical plate with constant heat flux and mass transfer.

In the above mentioned studies the effects of radiation on the flow has not been considered. Actually, many processes in new engineering areas occur at high temperature and knowledge of radiation heat transfer becomes imperative for the design of the pertinent equipment. Nuclear power plants, gas turbines and the various propulsion devices for aircraft, missiles, satellites, and space vehicles are examples of such engineering areas. The unsteady free convection flow past a vertical plate with chemical reaction under different temperature condition on the plate is elucidated by Neog *et al.*[10] and Rajesh *et al.*[11] Thermal radiation effect on the flow past a vertical plate with mass transfer is examined by Muralidharan *et al.*[12] and Rajput *et al.*[13]. Natural convective flow past an oscillating plate with constant mass flux in the presence of radiation has been studied by Chaudhary *et al.*[14]. The effects of radiation on free convection on the accelerated flow of a viscous incompressible fluid past an infinite vertical plate has many important technological applications in the astrophysical, geophysical and engineering problem. However, it seems that less attention was paid on hydromagnetic free convection flows near a vertical plate subjected to a constant heat flux boundary condition even though this situation involves in many engineering applications. Ogulu *et al.*[15] and Narahari *et al.*[16] have examined the flow past a surface with constant heat flux. The free convection effects on flow past an infinite vertical accelerated plate with constant heat flux is pioneered by Chaudhary *et al.*[17]. Ahmed and Dutta[18] have presented the transient mass transfer flow past an impulsively started infinite vertical plate with ramped plate velocity and ramped temperature.

The flow of fluid in the presence of natural convection is altered due to temperature and concentration gradient sultimately affecting the momentum boundary layer thickness.Wall suction and wall motion is an efficient way to control the thickness of momentum boundary layer. Besides this, electrically conducting fluid flow can be controlled by electromagnetic forces. Whereas, The motion of fluids with high electrical conductivity can be controlled by classical MHD flow control. In weakly conducting fluids however, the currents induced by an external magnetic field alone are too small, and an external electric field must be applied to achieve an efficient flow control. The study of effects of magnetic field on free convection flow is important in liquid metals, electrolytes and ionized gases. Geophysics encounters MHD phenomena in interaction on conducting fluids and magnetic fields. MHD in the present form is due to pioneer contribution of several notable authors like Alfven[19], Cowling[20]. With the advent of very high-speed (hypersonic) flight, the subject of magnetohydrodynamics (MHD) has assumed great significance. This is due to the fact that ahead of a high-speed body entering the atmosphere a shock wave, as mentioned earlier is formed between the wave and body surface and there will be a layer of gas at extremely high temperature due to shock compression as well as frictional heating in the boundary layer. At such high temperatures, the gas becomes ionized and hence becomes electrically conducting. Hence it can be expected that by the application of a suitably oriented magnetic field to the flow in the shock layer, the flow pattern can be modified and this in turn causes a change in the rate of heat transfer to the surface. When the ionized gas is sufficiently dense, the electron-atom collision frequency is large enough so that the tendency for the electrons to spiral around the magnetic field lines is suppressed.

It was emphasized by Cowling that when the strength of the applied magnetic field is sufficiently

large, Ohm's law needs to be modified to include Hall currents. The Hall effect is due merely to the sideways magnetic force on the drafting free charges. The electric field has to have a component transverse to the direction of the current density to balance this force. In many works of plasma physics, it is not paid much attention to the effect caused due to Hall current. However, the Hall effects can not be completely ignored if the strength of the magnetic field is strong and number of density of electrons is small as it is responsible for the change of the flow pattern of an ionized gas. Hall effect results in a development of an additional potential difference between opposite surfaces of a conductor for which a current is induced perpendicular to both the electric and magnetic field. This current is termed as Hall current. It was discovered in 1979 by Edwin Herbert Hall while working on his doctoral degree. Pop[21], Dutta *et al.*[22] and Malique and Sattar[23] have presented some model studies on the effect of Hall current on MHD convection flow because of its possible application in the problem of MHD generators and Hall current. Hall currents are of great importance in many astrophysical problems, Hall accelerator and flight MHD as well as flows of plasma in a MHD power generator (Alperin and Sutton[24]). Takhar *et al.*[25] have studied the unsteady free convection flow over an infinite vertical porous plate due to the combined effects of thermal and mass diffusion. The unsteady MHD free convective flow past a vertical porous plate immersed in a porous medium with Hall current, thermal diffusion and heat transfer has been studied by Ahmed *et al.*[26].

In all the above investigations, the analytical or numerical solution is obtained assuming that the temperature at the interface was continuous and well defined. However, there exist several problems of physical interest which may require non-uniform or arbitrary wall conditions. Seth *et al.*[27] have discussed the effect of rotation on unsteady hydromagnetic natural convection flow past an impulsively moving vertical plate with ramped temperature in a porous medium with thermal diffusion and heat absorption. Jana *et al.*[28, 29] have investigated the effects of rotation and radiation on the hydrodynamic flow past an impulsively started vertical plate with ramped plate temperature. The effects of radiation on MHD natural convection near a vertical plate with oscillatory ramped plate temperature have been presented by Jana *et al.*[30]. Sarkar *et al.*[31] have analyzed the effects of Hall currents and radiation on MHD free convective flow past an oscillating vertical plate with oscillatory plate temperature in a porous medium. The effect of radiation on MHD free convection flow past an impulsively moving vertical plate with ramped wall temperature have been studied by Ghara *et al.*[32]. Manna *et al.*[33] have examined the effects of radiation on unsteady MHD free convective flow past an oscillating vertical porous plate embedded in a porous medium with oscillatory heat flux. Narahari[34] has studied the transient free convection flow between long vertical parallel plates with ramped wall temperature at one boundary in the presence of thermal radiation and constant mass diffusion. Ahmed and Das[35] have examined the Hall effects on transient MHD flow past an impulsively started vertical plate in a porous medium with ramped temperature, rotation and heat absorption. Nandkeolyar *et al.*[36] have examined the unsteady hydromagnetic heat and mass transfer flow of a heat radiating and chemically reactive fluid past a flat porous plate with ramped wall temperature. The effects of thermal radiation and rotation on unsteady hydromagnetic free convection flow past an impulsively moving vertical plate with ramped temperature in a porous medium have been studied by Seth *et al.*[37]. Ahmed *et al.*[38] have presented the effects of Chemical reaction and radiation on an unsteady MHD flow past an accelerated infinite vertical plate with variable temperature and mass transfer. Seth *et al.*[39] have examined the effects of Hall current, radiation and rotation on natural convection heat and mass transfer flow past a moving vertical plate. An MHD natural convection heat and mass transfer flow past a time dependent moving vertical plate with ramped temperature in a rotating medium with Hall currents, radiation and chemical reaction has been described by Seth and Sarkar[40]. Seth *et al.*[41] have investigated the Soret and Hall effects on an unsteady MHD free convection flow of radiating and chemically reactive fluid past a moving vertical plate with ramped temperature in rotating system. Hayat *et al.*[42] have examined the influences of Hall current and chemical reaction in mixed convective peristaltic flow of Prandtl fluid. Hayat *et al.*[43] have analyzed the Hall and ion slip effects on peristaltic flow of Jeffrey nanofluid with Joule heating.

The main purpose of the present investigation is to study the combined effect of Hall currents, thermal radiation and ramped wall temperature and mass concentration on an MHD free convective flow past a moving plate when a strong magnetic field is

imposed. The magnetic Reynolds number have assumed to be so small that the induced magnetic field can be neglected. Rosseland model of radiation has been chosen in the investigation. The non-dimensional equations governing the flow are solved by the Laplace transform technique. Solutions are in terms of exponential and complementary error function. The results obtained in this work are consistent with the physical situation of the problem.

2 Formulation of the Problem

Consider the unsteady hydromagnetic flow of a viscous incompressible electrically conducting and heat radiating fluid past an impulsively moving infinite vertical plate with ramped plate temperature and mass transfer where a uniform magnetic field $\vec{B}$ of strength B_0 is applied in the direction perpendicular to the fluid flow. Choose a Cartesian co-ordinate system with the x - axis along the plate in the vertically upward direction, the y - axis perpendicular to the plate and z - axis is the normal of the xy -plane. The physical model of the problem is presented in Fig. 1. Initially, at time $t \le 0$, the plate and the fluid are at rest at a uniform temperature T_∞ and species concentration C_∞. At time $t > 0$, the plate at $y = 0$ starts to move in its own plane with a uniform velocity u_0 and the temperature of the plate at $y = 0$ is raised or lowered to $T_w + (T_w - T_\infty)\frac{t}{t_0},\ T_w \neq T_\infty$ and also the mass concentration at the plate $y = 0$

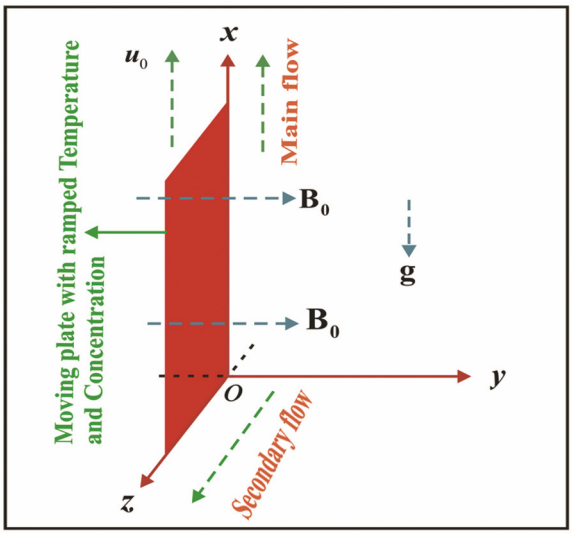

Fig. 1—Geometry of the problem

raised or lowered to $C_w + (C_w - C_\infty)\frac{t}{t_0},\ C_w \neq C_\infty$ when $0 < t \le t_0$ and the uniform temperature T_w and uniform mass concentration C_w are maintained when $t > t_0$. It is assumed that the flow is laminar and is such that the effects of the convective and pressure gradient terms in the momentum and energy equations can be neglected. It is also assumed that the radiative heat flux in the x - direction is negligible as compared to that in the y - direction. As the plate is of infinite extent and electrically nonconducting, all physical quantities, except the pressure, are functions of y and t only.

Generalized Ohm's law on taking Hall current into account is (Cowling[20]):

$$\vec{J} + \frac{\omega_e \tau_e}{B_0}\left(\vec{J} \times \vec{B}\right) = \sigma\left(\vec{E} + \vec{q} \times \vec{B}\right), \qquad \ldots (1)$$

where $\vec{q}$, $\vec{B}$, $\vec{E}$, $\vec{J}$, σ, ω_e and τ_e are respectively the velocity vector, the magnetic field vector, the electric field vector, the current density vector, electric conductivity, cyclotron frequency and electron collision time. In writing the Eq. (1), the ion-slip and the thermoelectric effects as well as the electron pressure gradient are neglected. The right hand side is the electric field in the moving frame. The first term on the left hand side comes from the electron drag on the ions. The second term is the Hall term and has to do with the idea that electrons and ions can decouple and move separately.

The equation of continuity $\nabla \cdot \vec{q} = 0$ with no-slip condition at the plate gives $v = 0$ everywhere in the flow where $\vec{q} \equiv (u, v, w)$, u, v and w are respectively velocity components along the coordinate axes. The fluid is a metallic liquid whose magnetic Reynolds number is small and hence the induced magnetic field produced by the fluid motion is negligible in comparison to the applied one[44] so that the magnetic field $\vec{B} \equiv (0, B_y, 0)$. The solenoidal relation $\nabla \cdot \vec{B} = 0$ gives $B_y = \text{constant} = B_0$ everywhere in the flow. The conservation of electric current $\nabla \cdot \vec{J} = 0$ yields $j_y =$ constant where $\vec{J} \equiv \left(j_x, j_y, j_z\right)$. This constant is zero since $j_y = 0$ at the plate which is electrically non-conducting. Hence, $j_y = 0$ everywhere in the flow.

In view of the above assumption, Eq. (1) yields:

$$j_x - m j_z = \sigma(E_x - w B_0), \qquad \ldots (2)$$

$$j_z + m j_x = \sigma(E_z + u B_0), \qquad \ldots (3)$$

where $m = \omega_e \tau_e$ is the Hall parameter which represets the ratio of electron-cyclotron frequency and the electron-atom collision frequency. In general, Hall currents influence the mechanics of a flow system when applied magnetic field is strong or when the collision frequency is low .The effect of Hall currents gives rise to a force in the y-direction, which induces a cross flow in that direction. To simplify the problem, we assume that there is no variation of flow quantities in y-direction. This assumption is considered to be valid if the surface be of infinite extent in the y-direction. Here $m \to \infty$ gives the result of the hydrodynamic fluid case and $m = 0$ corresponds to a MHD fluid in the absence of Hall currents.

Since the induced magnetic field is neglected, Maxwell's equation $\nabla \times \vec{E} = -\frac{\partial \vec{H}}{\partial t}$ becomes $\nabla \times \vec{E} = 0$ which gives $\frac{\partial E_x}{\partial y} = 0$ and $\frac{\partial E_z}{\partial y} = 0$. This implies that $E_x =$ constant and $E_z =$ constant everywhere in the flow. We choose this constants equal to zero, i.e. $E_x = E_z = 0$.

Solving for j_x and j_z from (2) and (3), on taking $E_x = E_z = 0$, we have:

$$j_x = \frac{\sigma B_0}{1+m^2}(mu - w), \qquad \ldots (4)$$

$$j_z = \frac{\sigma B_0}{1+m^2}(mw + u). \qquad \ldots (5)$$

Taking into consideration the assumptions made above, the governing equations for laminar natural convection flow of a viscous incompressible and electrically conducting fluid with radiative heat transfer, under Boussinesq approximation, i.e. the density changes with temperature, which gives rise to the buoyancy force, and using (4) and (5), are given by:

$$\frac{\partial u}{\partial t} = \nu \frac{\partial^2 u}{\partial y^2} - \frac{\sigma B_0^2}{\rho(1+m^2)}(u + mw) + g\beta(T - T_\infty) + g\beta^*(C - C_\infty), \qquad \ldots (6)$$

$$\frac{\partial w}{\partial t} = \nu \frac{\partial^2 w}{\partial y^2} + \frac{\sigma B_0^2}{\rho(1+m^2)}(mu - w), \qquad \ldots (7)$$

$$\rho c_p \frac{\partial T}{\partial t} = k \frac{\partial^2 T}{\partial y^2} - \frac{\partial q_r}{\partial y}, \qquad \ldots (8)$$

$$\frac{\partial C}{\partial t} = D \frac{\partial^2 C}{\partial y^2}, \qquad \ldots (9)$$

Where u is the velocity in the x-direction, T the temperature of the fluid, g the acceleration due to gravity, ν the kinematic viscosity, ρ the fluid density, k the thermal conductivity, C is concentration in the fluid, D is mass diffusivity, β the thermal expansion coefficient, β^* the concentration expansion coefficient, c_p the specific heat at constant pressure and q_r the radiative heat flux. The heating due to viscous dissipation is neglected for small velocities in the energy Eq. (9).

Assuming that there is no-slip between the plate and the fluid, the initial and boundary conditions for the fluid flow problem are:

$$t \le 0 : u = 0,\ w = 0,\ T = T_\infty,\ C = C_\infty \ \text{for}\ y \ge 0,$$

$$t > 0 : u = u_0,\ w = 0,\ T = \begin{cases} T_w + (T_w - T_\infty)\dfrac{t}{t_0} & \text{for } 0 < t \le t_0 \\ T_w & \text{for } t > t_0 \end{cases} \qquad \ldots (10)$$

$$C = \begin{cases} C_w + (C_w - C_\infty)\dfrac{t}{t_0} & \text{for } 0 < t \le t_0 \\ C_w & \text{for } t > t_0 \end{cases} \ \text{at}\ y = 0, \qquad \ldots (11)$$

$$t > 0 : u \to 0,\ w \to 0,\ T \to T_\infty,\ C \to C_\infty \ \text{at}\ y \to \infty.$$

In order to simplify the physical problem, the optically thick radiation limit is considered in the present analysis. For an optically thick fluid, in addition to emission there is also self-absorption and usually the absorption coefficient is wavelength dependent and large so that we can adopt the Rosseland approximation for radiative flux q_r. The radiative flux vector q_r under the Rosseland approximation is:

$$q_r = -\frac{4\sigma^*}{3k^*}\frac{\partial T^4}{\partial y}, \qquad \ldots (12)$$

where σ^* is the Stefan-Boltzman constant and k^* the spectral mean absorption coefficient of the medium. Assuming a small temperature difference between the fluid temperature T and the free stream temperature

T_∞, T^4 is expanded in a Taylor series about the free stream temperature T_∞. Neglecting second and higher order terms in $(T-T_\infty)$, we obtain:

$$T^4 = 4T_\infty^3 T - 3T_\infty^4. \quad \ldots (13)$$

It is emphasized here that Eq. (13) is widely used in computational fluid dynamics involving radiation absorption problems in expressing the term T^4 as a linear function.

In view of (12) and (13), Eq. (8) reduces:

$$\rho c_p \frac{\partial T}{\partial t} = k\frac{\partial^2 T}{\partial y^2} + \frac{16\sigma^* T_\infty^3}{3k^*}\frac{\partial^2 T}{\partial y^2}. \quad \ldots (14)$$

Introducing non-dimensionless variables:

$$\eta = \frac{u_0 y}{\nu}, \tau = \frac{t u_0^2}{\nu}, \ (u_1, w_1) = \frac{(u,w)}{u_0}, \theta = \frac{T-T_\infty}{T_w - T_\infty}, \ \phi = \frac{C-C_\infty}{C_w - C_\infty}, \quad \ldots (15)$$

Eqs. (6), (7), (9) and (14) become:

$$\frac{\partial u_1}{\partial \tau} = \frac{\partial^2 u_1}{\partial \eta^2} - \frac{M^2}{1+m^2}(u_1 + m w_1) + Gr\theta + Gc\phi, \quad \ldots (16)$$

$$\frac{\partial w_1}{\partial \tau} = \frac{\partial^2 w_1}{\partial \eta^2} + \frac{M^2}{1+m^2}(m u_1 - w_1), \quad \ldots (17)$$

$$3R \ \mathrm{Pr}\frac{\partial \theta}{\partial \tau} = (3R+4)\frac{\partial^2 \theta}{\partial \eta^2}, \quad \ldots (18)$$

$$\mathrm{Sc}\frac{\partial \phi}{\partial \tau} = \frac{\partial^2 \phi}{\partial \eta^2}, \quad \ldots (19)$$

where $M^2 = \frac{\sigma B_0^2 \nu}{\rho u_0^2}$ is the magnetic parameter which is the ratio of Lorentz force to viscous force, $\mathrm{Gr} = \frac{g\beta(T_w - T_\infty)\nu}{u_0^3}$ the thermal Grashof number characterrizes the relative effect of the thermal buoyancy force to the viscous hydrodynamic force, $\mathrm{Gc} = \frac{g\beta(C_w - C_\infty)\nu}{u_0^3}$ the mass Grashof number determines the relative effect of the species buoyancy force to the viscous hydrodynamic force, $R = \frac{k k^*}{4\sigma^* T_\infty^3}$ is the radiation parameter, $\mathrm{Pr} = \frac{\rho \nu c_p}{k}$ the Prandtl number that measurses ratio of momentum diffusivity to the thermal diffusivity, $\mathrm{Sc} = \frac{\nu}{D}$ the Schmidt number which embodies the ratio of thermal diffusivity to mass diffusivity.

Combining (16) and (17), we have:

$$\frac{\partial F}{\partial \tau} = \frac{\partial^2 F}{\partial \eta^2} - \frac{M^2(1-im)}{1+m^2}F + Gr\theta + Gc\phi, \quad \ldots (20)$$

where

$$F = u_1 + i w_1 \ \text{ and } \ i = \sqrt{-1}. \quad \ldots (21)$$

The corresponding initial and boundary conditions are:

$$F = 0, \ \phi = 0, \ \theta = 0 \ \text{ for all } \ \eta \ \text{ and } \ \tau \le 0,$$

$$F = 1, \ \phi = \begin{cases} \tau & \text{for } \ 0 < \tau \le 1 \\ 1 & \text{for } \ \tau > 1 \end{cases}, \ \theta = \begin{cases} \tau & \text{for } \ 0 < \tau \le 1 \\ 1 & \text{for } \ \tau > 1 \end{cases}$$

$$\text{at } \ \eta = 0 \quad \ldots (22)$$

$$F \to 0, \ \phi \to 0, \ \theta \to 0 \ \text{ at } \ \eta \to \infty \ \text{ for } \ \tau > 0.$$

On the use of the Laplace transformation, Eqs. (20), (18) -(19) become:

$$s\bar{F} = \frac{d^2 \bar{F}}{d\eta^2} - \frac{M^2(1-im)}{1+m^2}\bar{F} + \mathrm{Gr}\,\bar{\theta} + \mathrm{Gc}\,\bar{\phi}, \quad \ldots (23)$$

$$3R \ \mathrm{Pr}\, s\,\bar{\theta} = (3R+4)\frac{d^2 \bar{\theta}}{d\eta^2}, \quad \ldots (24)$$

$$s \ \mathrm{Sc}\,\bar{\phi} = \frac{d^2 \bar{\phi}}{d\eta^2}, \quad \ldots (25)$$

where

$$\bar{F}(\eta, s) = \int_0^\infty F(\eta,\tau)e^{-s\tau}d\tau, \ \bar{\theta}(\eta, s) = \int_0^\infty \theta(\eta,\tau)e^{-s\tau}d\tau,$$

$$\bar{\phi}(\eta, s) = \int_0^\infty \phi(\eta,\tau)e^{-s\tau}d\tau \quad \ldots (26)$$

and $s > 0$ (s being Laplace transform parameter).

The corresponding boundary conditions for $\bar{u}_1$, $\bar{\theta}$ and $\bar{\varphi}$ are:

$$\bar{F} = \frac{1}{s}, \ \bar{\theta} = \frac{1}{s^2}(1-e^{-s}), \ \bar{\phi} = \frac{1}{s^2}(1-e^{-s}) \ \text{ at } \ \eta = 0,$$

$$\bar{F} \to 0, \ \bar{\theta} \to 0, \ \bar{\phi} \to 0 \ \text{ at } \ \eta \to \infty. \quad \ldots (27)$$

The solution of Eqs. (23)-(25) subject to the boundary conditions (27) are easily obtained and are given by:

$$\bar{\phi}(\eta,s)=\frac{1}{s^2}(1-e^{-s})\,e^{-\sqrt{s\,\mathrm{Sc}}\,\eta}, \qquad \ldots (28)$$

$$\bar{\theta}(\eta,s)=\frac{1}{s^2}(1-e^{-s})\,e^{-\sqrt{s\,\alpha}\,\eta}, \qquad \ldots (29)$$

$$\bar{F}(\eta,s)=\begin{cases}\dfrac{e^{-\sqrt{s+a^2}\,\eta}}{s} \\ +\dfrac{1-e^{-s}}{s^2}\left[\dfrac{\mathrm{Gr}}{(\alpha-1)(s-\beta_0)}\left\{e^{-\sqrt{s+a^2}\,\eta}-e^{-\sqrt{\alpha s}\,\eta}\right\}\right. \\ \left.+\dfrac{\mathrm{Gc}}{(\mathrm{Sc}-1)(s-\gamma)}\left\{e^{-\sqrt{s+a^2}\,\eta}-e^{-\sqrt{\mathrm{Sc}\,s}\,\eta}\right\}\right] & \text{for } \alpha\neq 1,\ \mathrm{Sc}\neq 1, \\ \dfrac{e^{-\sqrt{s+a^2}\,\eta}}{s} \\ +\dfrac{1-e^{-s}}{s^2}\left[\dfrac{\mathrm{Gr}}{(\alpha-1)(s-\beta_0)}\left\{e^{-\sqrt{s+a^2}\,\eta}-e^{-\sqrt{\alpha s}\,\eta}\right\}\right. \\ \left.-\dfrac{\mathrm{Gc}}{a^2 s^2}\left\{e^{-\sqrt{s+a^2}\,\eta}-e^{-\sqrt{s}\,\eta}\right\}\right] & \text{for } \alpha\neq 1,\ \mathrm{Sc}=1,\end{cases}$$

$$\ldots (30)$$

where $\alpha=\dfrac{3RPr}{3R+4}$, $a^2=\dfrac{M^2(1-im)}{1+m^2}$, $\beta_0=\dfrac{a^2}{\alpha-1}$ and $\gamma=\dfrac{a^2}{\mathrm{Sc}-1}$.

The inverse transforms of (28)-(30) give the solution for the mass concentration, temperature distribution and velocity field as:

$$\varphi(\eta,\tau)=f_1(\eta\sqrt{\mathrm{Sc}},\tau)-H(\tau-1)\,f_1(\eta\sqrt{\mathrm{Sc}},\tau-1), \qquad \ldots (31)$$

$$\theta(\eta,\tau)=f_1(\eta\sqrt{\alpha},\tau)-H(\tau-1)f_1(\eta\sqrt{\alpha},\tau-1), \qquad \ldots (32)$$

$$F(\eta,\tau)=\begin{cases}f_2(\eta,\tau)+\dfrac{\mathrm{Gr}}{\alpha-1}\Big[f_3(\eta,\beta_0,\tau)-f_4(\eta\sqrt{\alpha},\beta_0,\tau) \\ -H(\tau-1)\{f_3(\eta,\beta_0,\tau-1)-f_4(\eta\sqrt{\alpha},\beta_0,\tau-1)\}\Big] \\ +\dfrac{\mathrm{Gc}}{\mathrm{Sc}-1}\Big[f_3(\eta,\gamma,\tau)-f_4(\eta\sqrt{Sc},\gamma,\tau) \\ -H(\tau-1)\{f_3(\eta,\gamma,\tau-1)-f_4(\eta\sqrt{Sc},\gamma,\tau-1)\}\Big] & \text{for } \alpha\neq 1,\ \mathrm{Sc}\neq 1, \\ f_2(\eta,\tau)+\dfrac{\mathrm{Gr}}{\alpha-1}\Big[f_3(\eta,\beta_0,\tau)-f_4(\eta\sqrt{\alpha},\beta_0,\tau) \\ -H(\tau-1)\{f_3(\eta,\beta_0,\tau-1)-f_4(\eta\sqrt{\alpha},\beta_0,\tau-1)\}\Big] \\ -\dfrac{Gc}{a^2}\big[f_5(\eta,a,\tau)-f_1(\eta,\tau) \\ -H(\tau-1)\{f_5(\eta,a,\tau-1)-f_1(\eta,\tau-1)\}\big] & \text{for } \alpha\neq 1,\ \mathrm{Sc}=1,\end{cases}$$

$$\ldots (33)$$

where f_1, f_2, f_3, f_4 and f_5 are dummy functions which are given in Appendix A, $\mathrm{erfc}(\xi)$ being complementary error function and and $H(\xi)$ is the unit step function.

2.1 Solution when Prandtl number is unity

In the absence of thermal radiation (i.e. when $R\to\infty$), i.e. if pure convection prevails, it is observed that $\alpha=\mathrm{Pr}$ and the solution for the temperature given by Eq. (31) is valid for all values of Pr, but the solution for the velocity field given by Eq. (33) is not valid for $\mathrm{Pr}=1$. Since the Prandtl number is a measure of the relative importance of the viscosity and thermal conductivity of the fluid, the case $\mathrm{Pr}=1$ corresponds to those fluids whose momentum and thermal boundary layer thicknesses are of the same order of magnitude. Therefore, the solution for the velocity field in the absence of thermal radiation effects when $\mathrm{Pr}=1$ has to be obtained subject to the initial and boundary conditions (22). It can be expressed in the following form:

$$F(\eta,\tau)=\begin{cases}f_2(\eta,\tau)+\dfrac{\mathrm{Gr}}{\mathrm{Pr}-1}\Big[f_3(\eta,\beta_0,\tau)-f_4(\eta\sqrt{\mathrm{Pr}},\beta_0,\tau) \\ -H(\tau-1)\{f_3(\eta,\beta_0,\tau-1)-f_4(\eta\sqrt{\mathrm{Pr}},\beta_0,\tau-1)\}\Big] \\ -\dfrac{\mathrm{Gc}}{a^2}\big[f_5(\eta,a,\tau)-f_1(\eta,\tau) \\ -H(\tau-1)\{f_5(\eta,a,\tau-1)-f_1(\eta,\tau-1)\}\big] & \text{for } Pr\neq 1,\ Sc=1 \\ f_2(\eta,\tau)-\dfrac{\mathrm{Gr}+\mathrm{Gc}}{a^2}\big[f_5(\eta,a,\tau)-f_1(\eta,\tau) \\ -H(\tau-1)\{f_5(\eta,a,\tau-1)-f_1(\eta,\tau-1)\}\big] & \text{for } Pr=1,\ Sc=1\end{cases}$$

$$\ldots (34)$$

where f_1, f_2, f_3, f_4 and f_5 are dummy functions which are given in Appendix A.

2.2 Solution for isothermal plate or constant plate temperature

In order to highlight the effect of the ramped boundary conditions on the flow, it may be worthwhile to compare such a flow past a moving plate with constant temperature. In this case, the initial and boundary conditions (22) are the same excepting the condition $\theta(0,\tau)=1$ and $\phi(0,\tau)=1$ for $\tau\geq 0$. Under the assumptions, it can be easily shown that the concentration, temperature and velocity fields for the flow past a moving plate with constant temperature can be expressed as:

$$\varphi(\eta,\tau)=\mathrm{erfc}\left(\frac{\eta}{2}\sqrt{\frac{\alpha}{\tau}}\right), \qquad \ldots (35)$$

$$\theta(\eta,\tau)=\operatorname{erfc}\left(\frac{\eta}{2}\sqrt{\frac{\mathrm{Sc}}{\tau}}\right), \qquad \ldots (36)$$

$$F(\eta,\tau)=f_2(\eta,\tau)+\frac{\mathrm{Gr}}{\alpha-1}\left[f_6(\eta,\beta_0,\tau)-f_7(\eta\sqrt{\alpha},\tau)\right] + \frac{\mathrm{Gc}}{\mathrm{Sc}-1}\left[f_6(\eta,\gamma,\tau)-f_7(\eta\sqrt{\mathrm{Sc}},\tau)\right] \text{ for } \alpha\neq 1,\ Sc\neq 1, \qquad \ldots (37)$$

where f_2, f_6 and f_7 are dummy functions which are given in Appendix *A*.

3 Results and Discussion

In this section, the obtained exact solutions are studied in order to determine the effects of embedded parameters. Numerical values of the non-dimensional fluid velocity components u_1 and w_1, fluid temperature θ, concentration ϕ for several values of magnetic parameter M^2, Hall parameter m, radiation parameter R, thermal Grashof number Gr, mass Grashof number Gc, Prandtl number Pr, Schmidt number Sc and time τ are presented in Figs. 2-14. The ghraphical results are presented using Mathematica.

3.1 Velocity profiles

Figure 2 shows the time evolution of the primary and secondary velocity profiles for a fixed set of parameter values. As shown in Fig. 2, to generate the plot, the values of η and τ are varied from 0 to 8 and 0 to 4, respectively. The surface plot helps to understand the variation in velocity components with η and τ. The value of the primary and secondary velocities is zero when η is close to 8 in both ramped temperature and isothermal cases. Also, the primary velocity enhances uniformly with time to its steady state value in both ramped temperature and isothermal cases, with the exception of the oscillatory behavior in the neighborhood of $\tau=1$. The secondary velocity enhances gradually and assume parabolic shape with time to its steady state value in both ramped temperature and isothermal cases, with the exception of the oscillatory behavior in the neighborhood of $\tau=1$. It is revealed from Fig. 3 the both primary and secondary velocities subpress as magnetic parameter M^2 increases in both ramped and isothermal cases. That is the primary or secondary fluid motion is retarded due to application of transverse magnetic field. This phenomenon clearly agrees to the fact that if an external magnetic force is applied perpendicular to the flow direction of an electrically conductive fluid, it experiences an electric field and produces current perpendicular to both magnetic field and flow direction. The product of electric current and

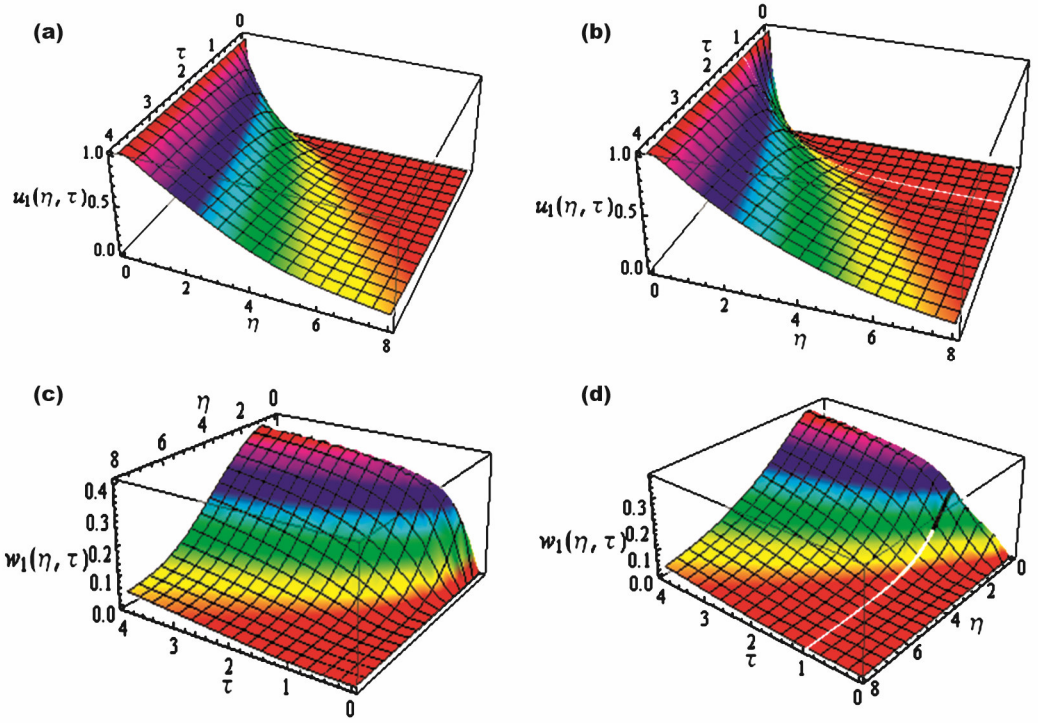

Fig. 2—Surface plot of primary and secondary velocities when $M^2=10$, $m=0.5$, $Pr=2$, $R=0.5$, $Gr=5$, $Gc=5$ and $Sc=0.23$

magnetic field creates a force which is known as Lorentz force. The direction of the Lorentz force is always opposite to the direction of fluid flow in the absence of an applied electric field. That is, the imposition of the transverse magnetic field is helpful in stabilizing the flow. Effects of Hall currents on velocity components are presented in Fig. 4. Both the primary and secondary velocities enhance when Hall parameter m increases in both ramped temperature and isothermal cases. It is attributed that larger values of Hall parameter m decrease the effective conductivity and thus decrease the magnetic damping force hence velocity components increase. In fact, the Hall effect balances the resistive influence of applied magnetic field to some extent. It is revealed form Fig. 5 that the both primary and secondary velocities decrease for incraing values of radiation parameter in both ramped and isothermal cases. This is consistent with the definition of R. An increase in the

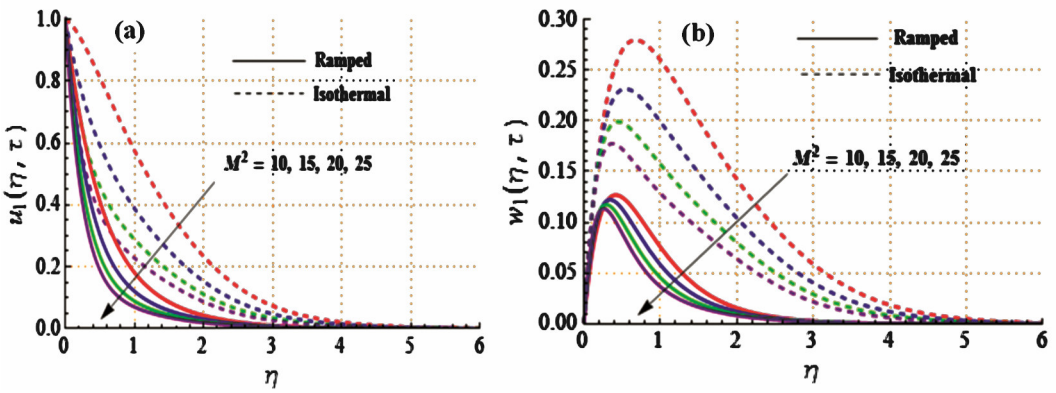

Fig. 3—Primary and secondary velocities for varying M^2 when $Pr = 2$, $m = 0.5$, $Gr = 5$, $Gr = 5$, $Sc = 0.23$ and $\tau = 0.5$

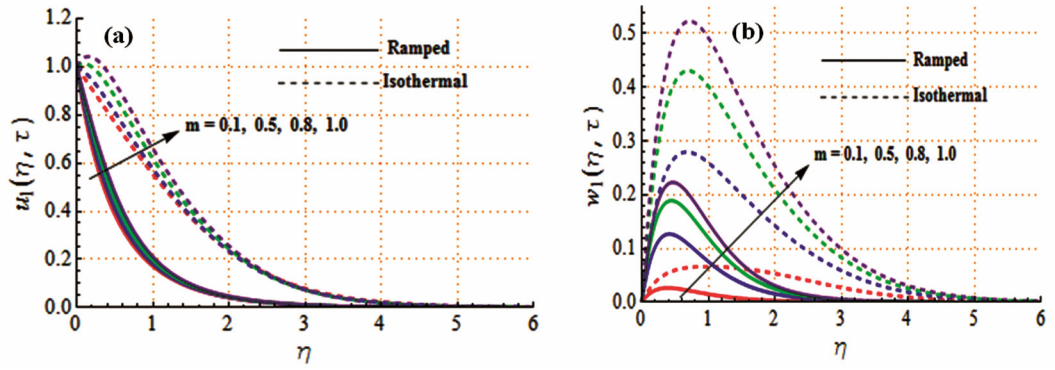

Fig. 4—Primary and secondary velocities for varying m when $M^2 = 10$, $Pr = 2$, $R = 0.5$, $Gr = 5$, $Gc = 5$, $Sc = 0.23$ and $\tau = 0.5$

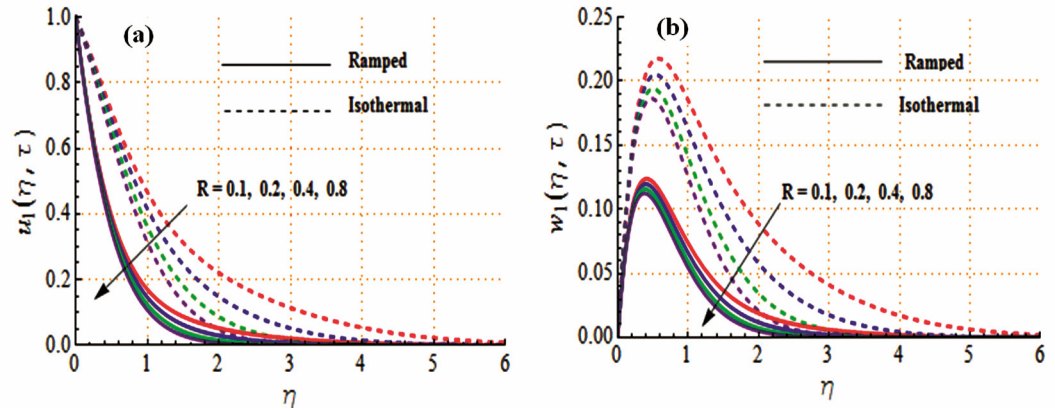

Fig. 5—Primary and secondary velocities for varying R when $M^2 = 10$, $Pr = 2$, $m = 0.5$, $Gr = 5$, $Gc = 5$, $Sc = 0.23$ and $\tau = 0.5$

value of R implies decreasing radiation effects. The case $R \to \infty$ represents the absence of thermal radiation i.e. the pure convection.

In Fig. 6, an increase in thermal Grashof number Gr leads to rise in fluid velocity components in both ramped and isothermal cases. Increasing thermal Grashoff number Gr decreases drag forces and hence velocity profiles increase. It is also noticed that fluid velocity components boost up very near the plate and after this fluid velocity components asymptotically decrease to its zero value as $\eta \to \infty$. This phenomenon is clearly supported by the physical reality, since the buoyancy effectcs are significant near the plate, which results in a sudden rise of the fluid velocity components adjacent to the plate. Fig. 7 elucidates the effects of mass Grashof number Gc on velocity components. The velocity components increase when mass Grashof number Gc increases in both ramped and isothermal cases. The mass Grashof number is defined as the ratio of the species buoyancy force to the viscous hydrodynamic force. As mass Grashof number increases, the viscous hydrodynamic force decreases. As a result, the momentum of the fluid is higher. Figure 8 shows that an increase in Schmidt number Sc leads to decrease in the fluid velocity components in both ramped and isothermal cases. We have chosen the Sc values as $Sc = 0.22$, 0.64, 1.20 and 2.23 which correspond to hydrogen, water vapor, sulfur dioxide and naphthalene respectively. Schmidt number shows the relative influence of momentum diffusion to species diffusion. Momentum diffusion is faster than species when $Sc > 1$ and opposite is true when $Sc < 1$. When $Sc =$ 1 both momentum and species diffuse at the same rate in the boundary layer. In this case both momentum and species boundary layers are of the same order of magnitude. As Sc increases velocity components are as expected reduced since increasingly momentum is diffused at a lesser rate than species.

As time progresses, the both primary and secondary velocities are getting accelerated shown in Fig. 9. This is due to increasing buoyancy effects as time progresses. From the above figures, it is noted that there is a significant difference can be observed between the velocity profiles due to ramped temperature and isothermal boundary conditions.

3.2 Temperature profiles

Figure 10 demonstrates the effects of of radiation parameter R, Prandtl number Pr and time on the

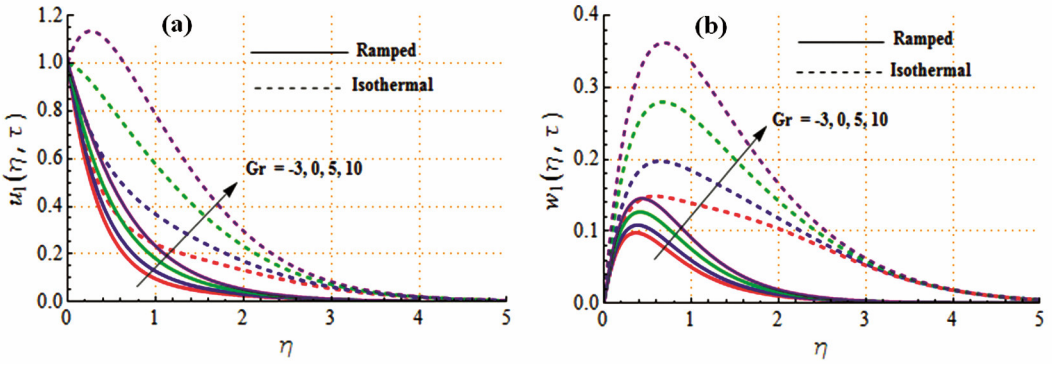

Fig. 6—Primary and secondary velocities for varying Gr when $M^2 = 10$, $R = 0.5$, $m = 0.5$, $Gc = 5$, $Sc = 0.23$ and $\tau = 0.5$

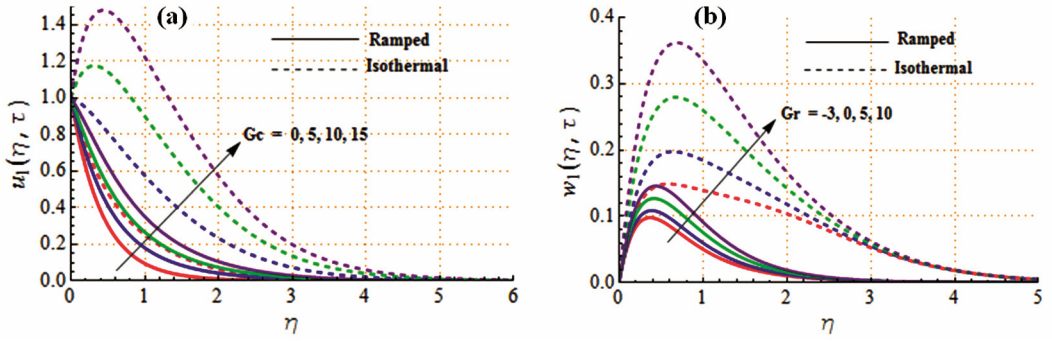

Fig. 7—Primary and secondary velocities for varying Gc when $M^2 = 10$, $Pr = 2$, $R = 0.5$, $Gr = 5$, $Sc = 0.23$ and $\tau = 0.5$

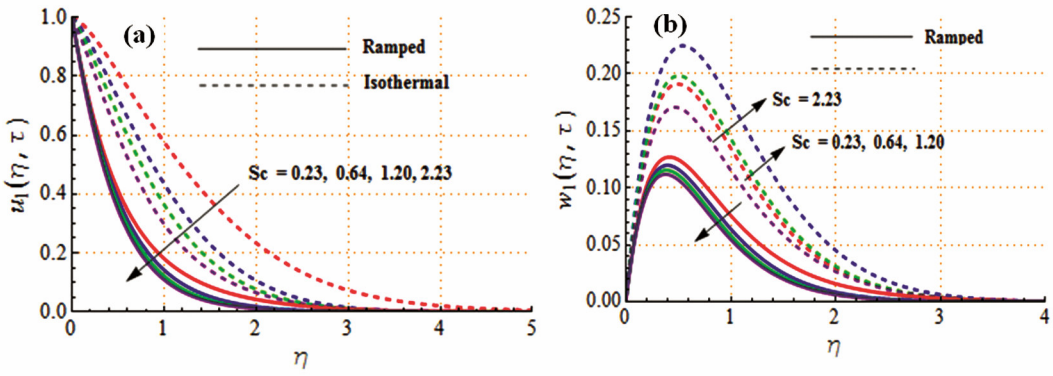

Fig. 8—Primary and secondary velocities for varying Sc when $M^2 = 10$, $Pr = 2$, $R = 0.5$, $Gr = 5$, $Gc = 5$, $m = 0.5$ and $\tau = 0.5$

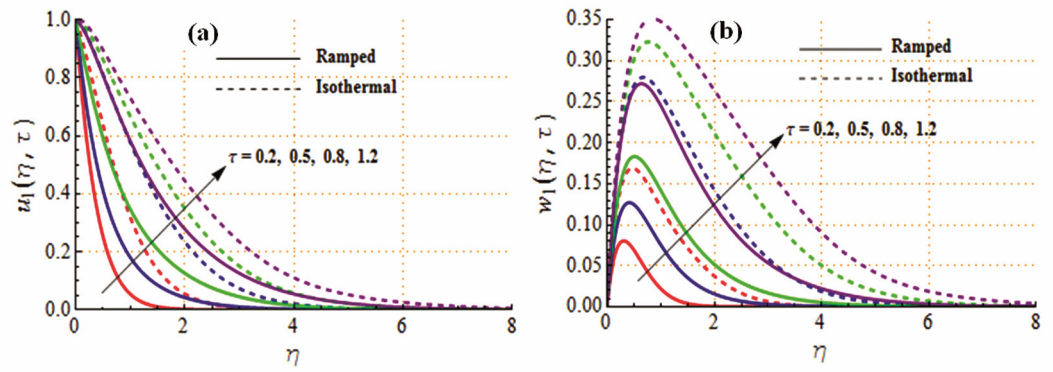

Fig. 9—Primary and secondary velocities for varying time τ when $M^2 = 10$, $Pr = 2$, $R = 0.5$, $Gr = 5$, $Gc = 5$, $Sc = 0.23$ and $m = 0.5$

fluid temperature distribution. Figure 10(a) elucidates that the fluid temperature θ decreases with an increase in radiation parameter R in both the ramped temperature and isothermal cases. In the presence of radiation, the thermal boundary layer always found to thicken which implies that the radiation provides an additional means to diffuse energy. This means that the thermal boundary layer decreases and more uniform temperature distribution across the boundary layer. Figure 10(b) shows the impact of Prandtl number on the temperature field θ. Prandtl number is the ratio of momentum to thermal diffusivities. Prandtl number has inverse relationship with thermal diffusivity. Increase in Prandtl number corresponds to stronger momentum diffusivity and weaker ther- mal diffusivity. Here weaker thermal diffusivity dominant over the stronger momentum diffusivity due to which lower temperature is noticed. Therefore, the temperature and thermal boundary layer thickness are decreased significantly when the values of Prandtl number are larged in both the ramped temperature and isothermal cases. The temperature θ increases in progess of time τ shown in Fig. 10(c). It is clear that the temperature profiles reach to unifrom temperature distribution due to increasing time in the case of isothermal boundary condition, but for the temperature profiles due to ramped boundary condition required more time to reach the unifrom temperature distribution.

3.3 Concentration profiles

This subsection deals with the variation in concentration profile ϕ for different values of embedded parameters. To be more realistic, the values of Schmidt number are chosen to represent the diffusing chemical species of most common interest like hydrogen ($Sc = 0.22$), water vapor ($Sc = 0.64$), sulfur dioxide ($Sc = 1.20$) and naphthalene ($Sc = 2.23$). The variations of Schmidt number Sc on species concentration are dreawn in Fig. 11(a). It is observed that the species concentration and the associated boundary layer decrease for an increase in Schmidt number Sc R in both the ramped concentration and isothermal

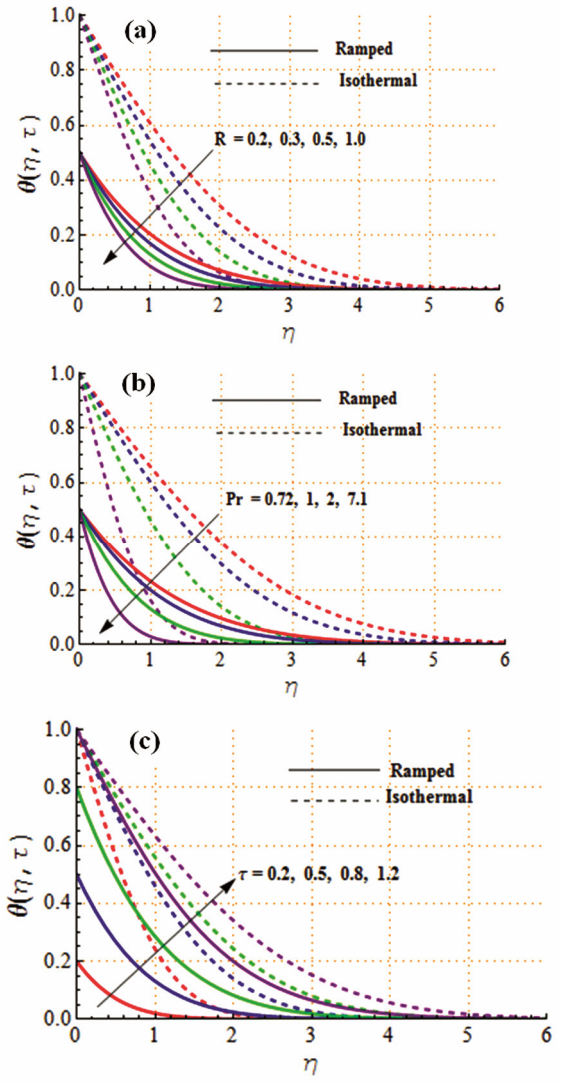

Fig. 10—Temperature profiles for varying (a) R when $Pr = 2$ and $\tau = 0.5$ (b) Pr when $R = 0.5$ and $\tau = 0.5$ (c) time τ when $Pr = 2$ and $R = 0.5$

cases. As larger values of Sc minimize the thermal diffusion and less diffused species prevents the fluid to become dense enough to enhance the concentration distribution and thus it drops with an increase in Schmidt number Sc. We recall that an increase in Schmidt number means a fall in mass diffusivity. This observation is in agreement with the outcome of Fig. 11(a). It is revealed from Fig. 11(b) that the concentration ϕ increases with an increase in time τ in both ramped concentration and isothermal cases. As time progresses, primary and secondary velocities are getting accelerated.

3.4 Rate of heat and mass transfer

In non-dimensional form, the rate of mass and heat transfers at the plate $\eta = 0$ are obtained as:

$$\phi_\eta(0,\tau) = \left(\frac{\partial \phi}{\partial \eta}\right)_{\eta=0} = -\sqrt{\frac{\mathrm{Sc}}{\pi}}\left[\tau^{1/2} - (\tau-1)^{1/2}\right], \qquad \ldots (38)$$

$$\theta_\eta(0,\tau) = \left(\frac{\partial \theta}{\partial \eta}\right)_{\eta=0} = -\sqrt{\frac{\alpha}{\pi}}\left[\tau^{1/2} - (\tau-1)^{1/2}\right]. \qquad \ldots (39)$$

For isothermal plate, the rate of mass and heat transfers at the plate $\eta = 0$ are given by:

$$\phi_\eta(0,\tau) = \left(\frac{\partial \phi}{\partial \eta}\right)_{\eta=0} = -\sqrt{\frac{\mathrm{Sc}}{\pi\tau}}, \qquad \ldots (40)$$

$$\theta_\eta(0,\tau) = \left(\frac{\partial \theta}{\partial \eta}\right)_{\eta=0} = -\sqrt{\frac{\alpha}{\pi\tau}} \qquad \ldots (41)$$

Numerical results of the rate of heat transfer $-\theta_\eta(0,\tau)$ at the plate $(\eta = 0)$ are presented in Fig. 12 for several values of radiation parameter R, Prandtl

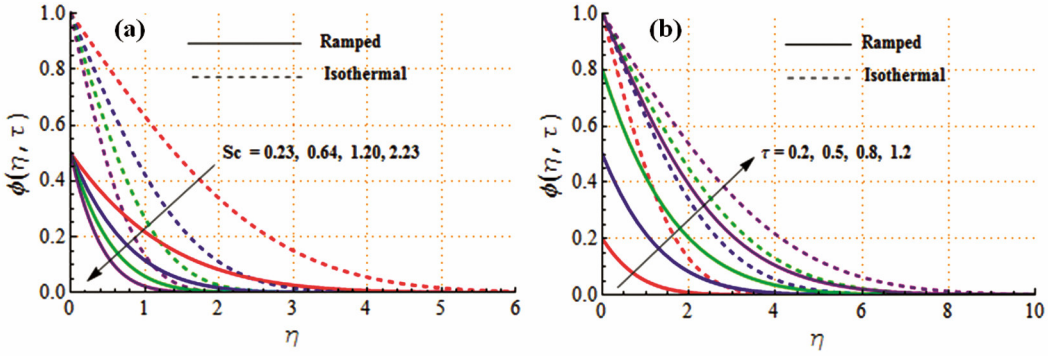

Fig. 11—Concentration profiles for varying (a) Sc when $\tau = 0.5$ (b) time τ when $Sc = 0.23$

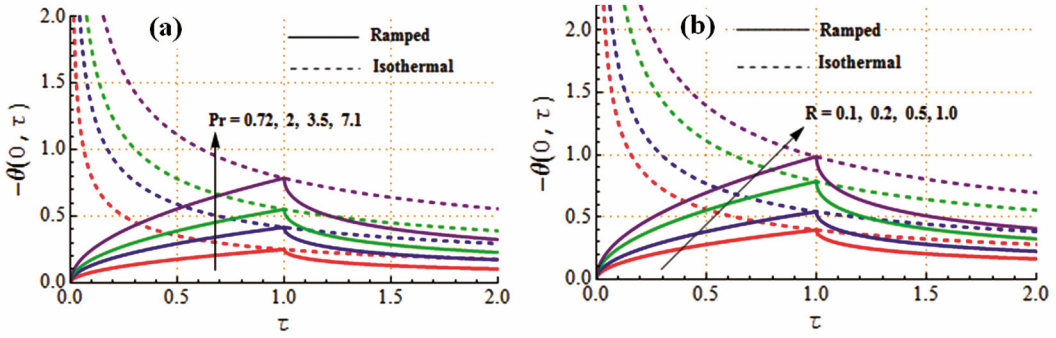

Fig. 12—Rate of heat transfer for varying (a) Pr when $\tau = 0.5$ (b) time τ when $Pr = 7.1$

number Pr and time τ. It is seen from Fig. 12(a) that the rate of heat transfer $-\theta_\eta(0,\tau)$ enhances when Prandtl number Pr increases. in both the ramped temperature and isothermal cases. Prandtl number is the ratio of momentum diffusivity to thermal diffusivity. It is a thermophysical property of a fluid. For the case $\mathrm{Pr} < 1$, thermal diffusivity exceeds momentum diffusivity. In other words, in this case heat will diffuse at a quicker rate than momentum. For the case $\mathrm{Pr} = 1$, the viscous and energy diffusion rates are the same i.e. the thermal and momentum boundary layers are of the same order of magnitude. For the case $\mathrm{Pr} > 1$, momentum diffusivity is greater than thermal diffusivity. In other words, momentum will diffuse at a quicker rate than heat.This is consistent with the fact that smaller values of Pr are equivalent to increasing thermal conductivities and therefore heat is able to diffuse away from the plate more rapidly than higher values of Pr, hence the rate of heat transfer at the plate is reduced. Fig. 12(b) reveals that the rate of heat transfer $-\theta_\eta(0,\tau)$ increases with an increase in radiation parameter R in both the ramped temperature and isothermal cases. Thus, the thermal radiation tends to accelerate heat transfer at the plate while thermal diffusion has the reverse effect. The rate of heat transfer $-\theta_\eta(0,\tau)$ is decreasing function of time for isothermal boundary condition, but it has increasing behavior for $\tau < 1$, an opposite behavior is observed for $\tau > 1$ in the case of ramped boundary condition. Moreover, there is a sharp rise in the rate of heat transfer $-\theta_\eta(0,\tau)$ in the neighborhood of $\tau = 1$ only in the case of ramped wall temperature. This is due to the transition of the temperature from ramped to isothermal at $\tau = 1$. This is an excellent agreement with Narahari[34]. Negative value of $\theta_\eta(0,\tau)$ means that the heat flows from the moving

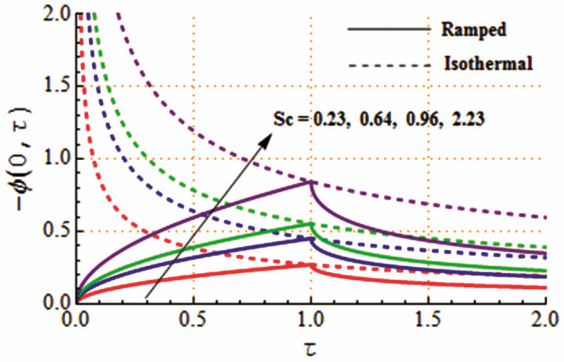

Fig. 13—Rate of mass transfer for varying Sc

plate to fluid. This is expected since the plate is hotter than the fluid.

The numerical results of the rate of mass transfer $-\phi_\eta(0,\tau)$ at the plate $(\eta = 0)$ are presented in Fig. 13 for several values of Schmidt number Sc and time τ. It can be seen from Fig. 13 that larger values of Sc enhanc the rate of mass transfer $-\phi_\eta(0,\tau)$ in both the ramped concentration and isothermal cases. Infact Schmidt number is the ratio of viscous diffusion rate to molecular diffusion rate. Therefore higher values of Schmidt number enhance the viscous diffusion rate which in turn increases the rate of mass transfer $-\phi_\eta(0,\tau)$. From Figs. 12 and 13, it is seen that the rate of heat and mass transfer is not presented at $\tau = 0$ in the isothermal case because $\tau = 0$ is a singular point, but the rate of heat and mass transfer is presented for all values of time in the case of ramped boundary condition because it is well defined at all τ.

3.5 Shear stresses

In non-dimensional form, the shear stresses at the plate $\eta = 0$ due to the fluid flows are given by:

$$\tau_x + i\,\tau_y = \left(\frac{\partial F}{\partial \eta}\right)_{\eta=0}$$

$$= \begin{cases} -f_8(a,\tau)+\dfrac{\mathrm{Gr}}{\alpha-1}\left[f_9(\beta_0,\tau)+f_{10}(\alpha,\beta_0,\tau)\right. \\ \left.-H(\tau-1)\{f_9(\beta_0,\tau-1)+f_{10}(\alpha,\beta_0,\tau-1)\}\right] \\ +\dfrac{\mathrm{Gc}}{\mathrm{Sc}-1}\left[f_9(\gamma,\tau)+f_{10}(\mathrm{Sc},\gamma,\tau)\right. \\ \left.-H(\tau-1)\{f_9(\gamma,\tau-1)+f_{10}(\mathrm{Sc},\gamma,\tau-1)\}\right] \quad \text{for } \alpha\neq 1,\ \mathrm{Sc}\neq 1, \\ \\ -f_8(a,\tau)+\dfrac{\mathrm{Gr}}{\alpha-1}\left[f_9(\beta_0,\tau)+f_{10}(\alpha,\beta_0,\tau)\right. \\ \left.-H(\tau-1)\{f_9(\beta_0,\tau-1)+f_{10}(\alpha,\beta_0,\tau-1)\}\right] \\ +\dfrac{\mathrm{Gc}}{a^2}\left[\left\{f_{11}(a,\tau)-2\sqrt{\dfrac{\tau}{\pi}}\right\}\right. \\ \left.-H(\tau-1)\left\{f_{11}(a,\tau-1)-2\sqrt{\dfrac{\tau-1}{\pi}}\right\}\right] \quad \text{for } \alpha\neq 1,\ \mathrm{Sc}=1, \end{cases}$$

... (42)

where f_6, f_7, f_8 and f_9 are dummy functions which are given in Appendix *A*.

For isothermal plate, the shear stresses at the plate $\eta=0$ due to the fluid flows:

$$\tau_x + i\,\tau_y = \left(\frac{\partial F}{\partial \eta}\right)_{\eta=0}$$

$$= -f_8(a,\tau)+\frac{\mathrm{Gr}}{\alpha-1}\left[f_{12}(\beta_0,\tau)-\frac{1}{\beta_0}f_8(a,\tau)+f_{13}(\alpha,\beta_0,\tau)\right]$$

$$+\frac{\mathrm{Gc}}{\mathrm{Sc}-1}\left[f_{12}(\gamma,\tau)-\frac{1}{\gamma}f_8(a,\tau)+f_{13}(\mathrm{Sc},\gamma,\tau)\right] \text{ for } \alpha\neq 1,\ \mathrm{Sc}\neq 1,$$

... (43)

where f_8, f_{12} and f_{13} are dummy functions which are given in Appendix *A*.

Numerical values of the non-dimensional shear stresses τ_x and τ_y due to the primary and secondary flows at the plate $\eta=0$ are presented in Figs. 14-20 for several values of magnetic parameter M^2, Hall parameter m, Grashof number Gr, mass Grashof number Gc, Schmidt number Sc and Prandtl number Pr. In Fig. 14, the magnetic parameter M^2 is found to elevate the shear stresses τ_x and τ_y in both ramped and isothermal cases, because the velocity gradient increases near the plate. Figure 15 shows that the

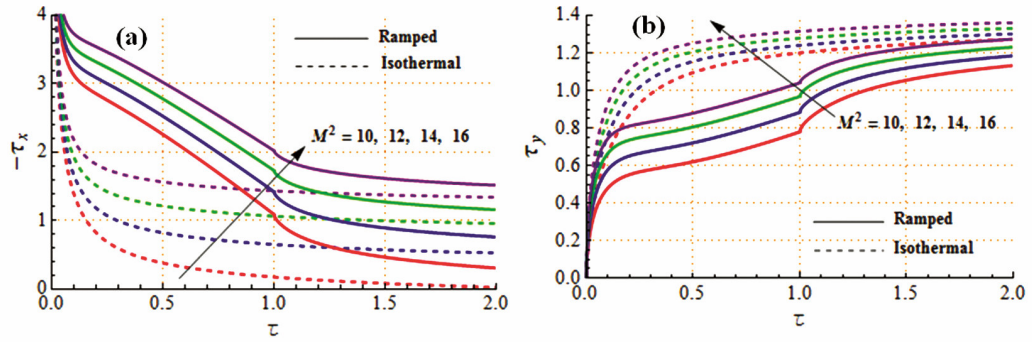

Fig. 14—Shear stresses τ_x and τ_y for varying M^2 when $R=0.5$, $Pr=7.1$, $m=0.5$, $Gr=5$, $Gc=5$ and $Sc=0.23$

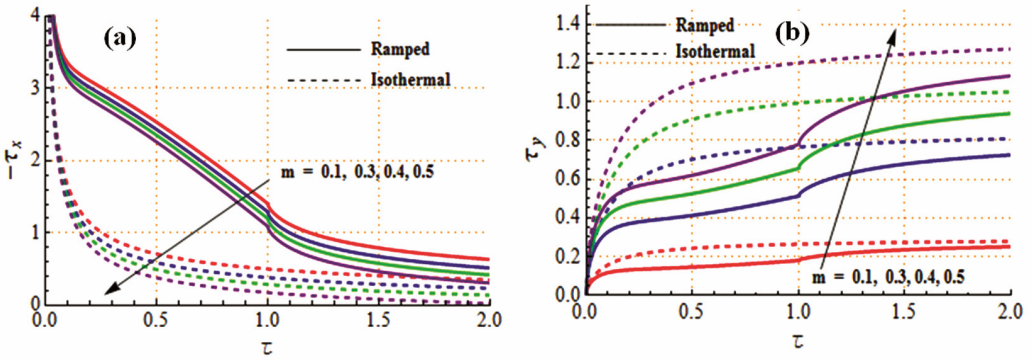

Fig. 15—Shear stresses τ_x and τ_y for varying m when $R=0.5$, $Pr=7.1$, $M^2=10$, $Gr=5$, $Gc=5$ and $Sc=0.23$

shear stresses τ_x and τ_y enhance when Hall parameter m is largered in both ramped temperature and isothermal cases. As radiation parameter R increases, the shear stresses τ_x and τ_y are reduced in both ramped and isothermal cases . This is due to the fact that an increase in R causes a decrease in the velocity components and hence the shear stresses at the plate reduce in both ramped and isothermal cases.

It is seen from Fig. 16 that the shear stresses τ_x and τ_y enhance when thermal Grashof number Gr enlarges in both ramped temperature and isothermal cases. Figure 17 reveals that the shear stresses τ_x and τ_y enhance for increasing values of mass Grashof number Gc in both ramped and isothermal cases. Figure 18 reveal that the shear stresses τ_x and τ_y decrease with an increase in Prandtl number Pr in

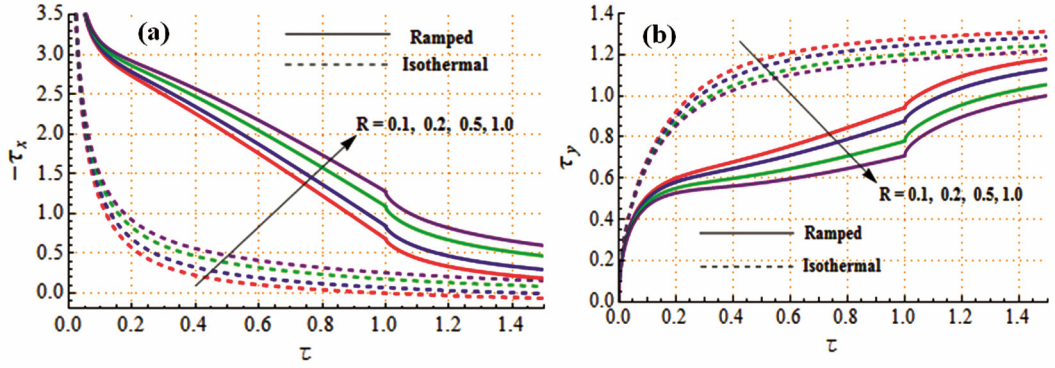

Fig. 16—Shear stresses τ_x and τ_y for varying R when $M^2 = 10$, $m = 0.5$, $Gr = 5$, $Gc = 5$, $Pr = 7.1$ and $Sc = 0.23$

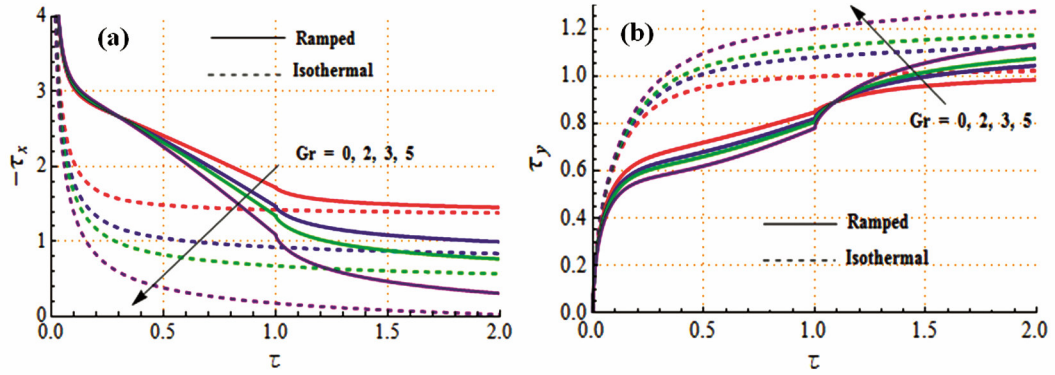

Fig. 17—Shear stresses τ_x and τ_y for varying Gr when $R = 0.5$, $Pr = 7.1$, $M^2 = 10$, $m = 0.5$, $Gc = 5$ and $Sc = 0.23$

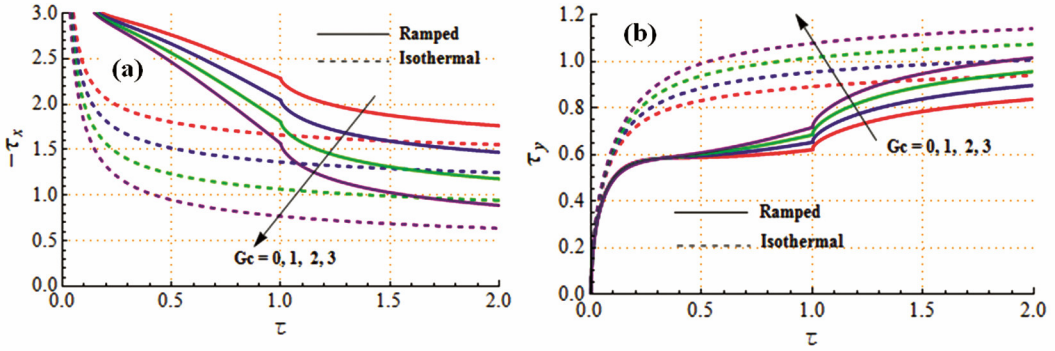

Fig. 18—Shear stresses τ_x and τ_y for varying Gc when $R = 0.5$, $Pr = 7.1$, $M^2 = 10$, $m = 0.5$, $Gr = 5$ and $Sc = 0.23$

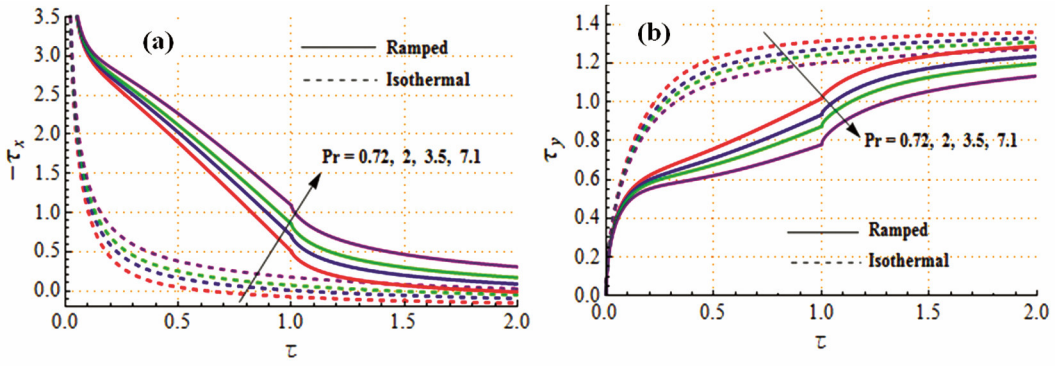

Fig. 19—Shear stresses τ_x and τ_y for varying Pr when $R = 0.5$, $Sc = 0.23$, $M^2 = 10$, $m = 0.5$, $Gr = 5$ and $Gc = 5$

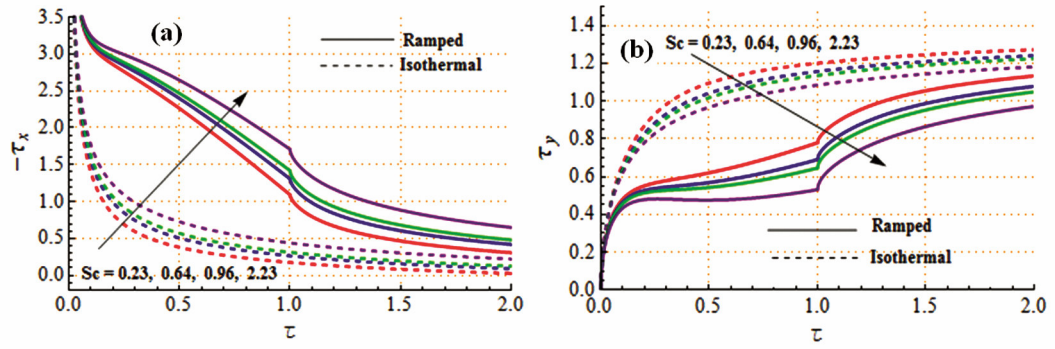

Fig. 20—Shear stresses τ_x and τ_y for varying Sc when $R = 0.5$, $Gc = 5$, $M^2 = 10$, $m = 0.5$, $Gr = 5$ and $Pr = 7.1$

both ramped and isothermal cases. This is consistent with the fact that an increase in the Prandtl number means an increase of fluid viscosity, which causes a decrease in shear stresses at the plate. From Fig. 19, it can be seen that the shear stresses τ_x and τ_y decrease when Schmidt number Sc increases in both ramped temperature and isothermal cases. The reason is due to the fact that the increase in Schmidt number causes a decrease in flow velocity and hence shear stresses reduce at the plate. It is interesting to note that the shear stresses τ_x and τ_y are increasing functions of time for isothermal boundary condition, but it has increasing behavior for $\tau < 1$, an opposite behavior is observed for $\tau > 1$ in the case of ramped boundary condition. There is a sharp rise in the shear stresses τ_x and τ_y in the neighborhood of $\tau = 1$ only in the case of ramped wall temperature. This is due to the transition of the temperature from ramped to isothermal at $\tau = 1$. Physically, negative value of the shear stress τ_x signifies the moving plate exerts a drag force on the fluid along x-axis, and positive value means the opposite. This is expected since in the present problem, we consider the case of a moving plate which induces the flow.

4 Conclusions

In this paper, the impacts of Hall effect, radiation and ramped wall temerature and mass concentration on the unsteady hydromagnetic free convective flow of a viscous incompressible electrically conducting and heat radiating fluid past an infinite vertical plate hasve been examined. The main findings obtained from the present study may be summarized as follows:

(i) The primary and secondary velocities are retarded under the effects of transverse magnetic field whereas these are accelerated due to Hall effects in both ramped temperature and isothermal cases.

(ii) An increase in either radiation parameter or thermal Grashof number or mass Grashof number leads to rise in the velocity components.

(iii) The fluid temperature decreases with an increase in radiation parameter. The fluid temperature increases when time progresses.

(iv) The shear stress at the plate enhances for increasing values of radiation parameter.
(v) The rate of heat transfer increases when radiation parameter enlarges.
(vi) Such a fluid flow finds many engineering applications such as those in MHD devices and in several natural phenomena occurring subject to thermal radiation in the presence of mass transfer.

References

1 Welty J R, Wicks C E, Wilson R E & Rorrer G L, *Fundamentals of momentum, heat mass Transfer*, (John Wiley and Sons, USA), 2007.
2 Cussler E L, *Diffusion mass transfer in fluid systems*, (Cambridge University Press, Cambridge),1998.
3 Chaudhary R C & Jain A, *Rom J Phys*, 52 (2007) 505.
4 Muthucumaraswamy R & Kumer G S, *Theor Appl Mech*, 31(1) (2004) 35.
5 Muthucumaraswamy R & Vijayalakshmi A, *Int J Appl Math Mech*, 4 (2008) 59.
6 Muthucumaraswamy R, Sundar R M & Subramanian V S A, *Int J Appl Math Mech*, 5 (2009) 51.
7 Rajput U S & Kumar S, *Appl Math Sci*, 5(3) (2011) 149.
8 Juncu Gh, *Heat Mass Transfer*, 41 (2005) 1095.
9 Das U N, Deka R K & Soundalgekar V M, *Forsch Ingenieurwes*, 60 (1994) 284.
10 Bhaben C N & Das R K, *Int J Eng Res Tech*, 1 (2012) 1.
11 Rajesh V, *Int J Appl Math Mech*, 6(14) (2010) 60.
12 Muralidharan M & Muthucumaraswamy R, *Indian J Sci Tech*, 3 (2010) 398.
13 Rajput U S & Kumar S, *Int J Appl Math Mech*, 8 (2012) 66.
14 Chaudhary R C & Jain A, *Acta Tech CSAV*, 52 (2007) 93.
15 Ogulu A & Makinde O D,*Chem Eng Commun*, 196 (2009) 454.
16 Narahari M & Debnath L, *Z Angew Math Mech*, 93, (2013) 38.
17 Chaudhary R C & Jain A, *Matematicas*, XVII (2009) 73.
18 Ahmed N & Dutta M, *Int J Phys Sci*, 8(7) (2013) 254.
19 Alfven H, *Nature,* 150 (1942) 405.
20 Cowling T G, *Magnetohydrodynamics*, (Wiley Inter Science, New York), 1957.
21 Pop I, *J Math Phys* Sci, 5 (1971) 375.
22 Datta N & Jana R N, *J Phys Soc Japan*, 40 (1976) 1469.
23 Malique M A & Sattar M A, *Int J Heat Mass Tran*, 48 (2005) 4963.
24 Alperin M & Sutton G P, *Advanced propulsion systems*, (Pergamon Press, New York), 1959.
25 Takhar H S, Roy S & Nath G, *Heat Mass Transfer*, 39(10) (2003) 825.
26 Ahmed N, Kalita H & Baruah D P, *Int J Eng Sci Technol*, 2(6) (2010) 59.
27 Seth G S, Nandkeolyar R & Ansari M S, *Int J Appl Math Mech*, 7(21) (2011) 52.
28 Jana M, Das S & Jana R N, *Int J Appl Info Syst*, 3(4) (2012) 39.
29 Jana M, Das S & Jana R N, *Int J Appl Eng*, 2 (2012) 170.
30 Jana M, Das S & Jana R N, *Int J Eng Innov Res*, 1(4) (2012) 366.
31 Sarkar B C, Das S & Jana R N, *Bull Soc Math Serv Stand*, 1(3) (2012) 06.
32 Ghara N, Das S, Maji S L & Jana R N, *Am J Sci Ind Res*, 3(6) (2012) 376.
33 Manna S S, Das S & Jana R N, *Adv Appl Sci Res*, 3(6) (2012) 3722.
34 Narahari, M, *Meccanica*, 47 (2012) 1961.
35 Ahmed N & Das K K, *Appl Math Sci*, 7(51) (2013) 2525.
36 Nandkeolyar R, Das M & Sibanda P, *Math Probl Eng*, 2013 (2013) 1.
37 Seth G S, Nandkeolyar R & Ansari M S, *J Appl Fluid Mech*, 6(1) (2013) 27.
38 Ahmed N, Goswami J K & Barua D P, *Indian J Pure Appl Math*, 44(4) (2013) 443.
39 Seth G S, Sarkar S & Hussain S M, *Ain Shams Eng J*, 5 (2014) 489.
40 Seth G S & Sarkar S, *J Mech*, 31(01) (2015) 91.
41 Seth G S, Kumbhakar B & Sarkar S, *Int J Eng Sci Technol,* 7(2) (2015) 94.
42 Hayat T, Zahir H, Tanveer A & Alsaedi A, *J Magn Magn Mater*, 407 (2016) 321.
43 Hayat T, Shafique M, Tanveer A & Alsaedi A, *J Magn Magn Mater*, 407 (2016) 51.
44 Cramer K & Pai S, *Magnetofluid dynamics for engineers and applied physicists*, (McGraw Hill, New York, USA), 1973.

Appendix A

The following constant expressions are utilized in the results:

$$f_1(\xi,\tau)=\left(\tau+\frac{1}{2}\xi^2\right)\operatorname{erfc}\left(\frac{\xi}{2\sqrt{\tau}}\right)-\sqrt{\frac{\tau}{\pi}}\,\xi\,e^{-\frac{\xi^2}{4\tau}},$$

$$f_2(\xi,\tau)=\frac{1}{2}\left[e^{a\xi}\operatorname{erfc}\left(\frac{\xi}{2\sqrt{\tau}}+a\sqrt{\tau}\right)+e^{-a\xi}\operatorname{erfc}\left(\frac{\xi}{2\sqrt{\tau}}-a\sqrt{\tau}\right)\right],$$

$$f_3(\xi,\lambda,\tau)=\frac{e^{\lambda\tau}}{2\lambda^2}\left[e^{\xi\sqrt{a^2+\lambda}}\operatorname{erfc}\left\{\frac{\xi}{2\sqrt{\tau}}+\sqrt{(a^2+\lambda)\tau}\right\}+e^{-\xi\sqrt{a^2+\lambda}}\operatorname{erfc}\left\{\frac{\xi}{2\sqrt{\tau}}-\sqrt{(a^2+\lambda)\tau}\right\}\right]$$

$$-\frac{1}{2\lambda}\left[\left(\tau+\frac{1}{\lambda}+\frac{\xi}{2a}\right)e^{a\xi}\operatorname{erfc}\left(\frac{\xi}{2\sqrt{\tau}}+a\sqrt{\tau}\right)+\left(\tau+\frac{1}{\lambda}-\frac{\xi}{2a}\right)e^{-a\xi}\operatorname{erfc}\left(\frac{\xi}{2\sqrt{\tau}}-a\sqrt{\tau}\right)\right],$$

$$f_4(\xi,\lambda,\tau)=\frac{e^{\lambda\tau}}{2\lambda^2}\left[e^{\xi\sqrt{\lambda}}\,\mathrm{erfc}\left(\frac{\xi}{2\sqrt{\tau}}+\sqrt{\lambda\tau}\right)+e^{-\xi\sqrt{\lambda}}\,\mathrm{erfc}\left(\frac{\xi}{2\sqrt{\tau}}-\sqrt{\lambda\tau}\right)\right]$$
$$+\frac{1}{2\lambda}\left[2\sqrt{\frac{\tau}{\pi}}\,\xi\,e^{-\frac{\xi^2}{4\tau}}-\xi^2\,\mathrm{erfc}\left(\frac{\xi}{2\sqrt{\tau}}\right)\right]-\frac{1}{\lambda}\left(\tau+\frac{1}{\lambda}\right)\mathrm{erfc}\left(\frac{\xi}{2\sqrt{\tau}}\right),$$

$$f_5(\xi,\lambda,\tau)=\frac{1}{2}\left[\left(\tau+\frac{\xi}{2\lambda}\right)e^{\lambda\xi}\,\mathrm{erfc}\left(\frac{\xi}{2\sqrt{\tau}}+\lambda\sqrt{\tau}\right)+\left(\tau-\frac{\xi}{2\lambda}\right)e^{-\lambda\xi}\,\mathrm{erfc}\left(\frac{\xi}{2\sqrt{\tau}}-\lambda\sqrt{\tau}\right)\right],$$

$$f_6(\xi,\lambda,\tau)=\frac{e^{\lambda\tau}}{2\lambda}\left[e^{\xi\sqrt{a^2+\lambda}}\,\mathrm{erfc}\left\{\frac{\xi}{2\sqrt{\tau}}+\sqrt{(a^2+\lambda)\tau}\right\}+e^{-\xi\sqrt{a^2+\lambda}}\,\mathrm{erfc}\left\{\frac{\xi}{2\sqrt{\tau}}-\sqrt{(a^2+\lambda)\tau}\right\}\right]$$
$$-\frac{1}{2\lambda}\left[e^{a\xi}\,\mathrm{erfc}\left(\frac{\xi}{2\sqrt{\tau}}+a\sqrt{\tau}\right)+e^{-a\lambda}\,\mathrm{erfc}\left(\frac{\xi}{2\sqrt{\tau}}-a\sqrt{\tau}\right)\right],$$

$$f_7(\xi,\lambda,\tau)=\frac{e^{\lambda\tau}}{2\lambda}\left[e^{\xi\sqrt{\lambda}}\,\mathrm{erfc}\left(\frac{\xi}{2\sqrt{\tau}}+\sqrt{\lambda\tau}\right)+e^{-\xi\sqrt{\lambda}}\,\mathrm{erfc}\left(\frac{\xi}{2\sqrt{\tau}}-\sqrt{\lambda\tau}\right)\right]-\frac{1}{\lambda}\,\mathrm{erfc}\left(\frac{\xi}{2\sqrt{\tau}}\right),$$

$$f_8(\lambda,\tau)=\lambda\,\mathrm{erf}\left(\lambda\sqrt{\tau}\right)+\frac{1}{\sqrt{\pi\tau}}\,e^{-\lambda^2\tau},$$

$$f_9(\lambda,\tau)=-\frac{e^{\lambda\tau}}{\lambda^2}\left[\sqrt{a^2+\lambda}\,\mathrm{erf}\left(\sqrt{(a^2+\lambda)\tau}\right)+\frac{1}{\sqrt{\pi\tau}}\,e^{-(a^2+\lambda)\tau}\right]$$
$$+\frac{1}{\lambda}\left[\left\{a\left(\tau+\frac{1}{\lambda}\right)+\frac{1}{2a}\right\}\mathrm{erf}\left(a\sqrt{\tau}\right)+\frac{1}{\sqrt{\pi\tau}}\left(\tau+\frac{1}{\lambda}\right)e^{-a^2\tau}\right],$$

$$f_{10}(\xi,\lambda,\tau)=\frac{e^{\lambda\tau}}{\lambda^2}\left[\sqrt{\lambda\xi}\;\mathrm{erf}\left(\sqrt{\lambda\tau}\right)+\frac{1}{\sqrt{\pi\tau}}\,e^{-\lambda\tau}\right]-\frac{1}{\lambda}\sqrt{\frac{\xi}{\pi\tau}}\left(3\tau+\frac{1}{\lambda}\right),$$

$$f_{11}(\lambda,\tau)=\left(\lambda\tau+\frac{1}{2\lambda}\right)\mathrm{erf}\left(\lambda\sqrt{\tau}\right)+\sqrt{\frac{\tau}{\pi}}\,e^{-\lambda^2\tau},$$

$$f_{12}(\lambda,\tau)=-\frac{e^{\lambda\tau}}{\lambda}\left[\sqrt{a^2+\lambda}\,\mathrm{erf}\left(\sqrt{(a^2+\lambda)\tau}\right)+\frac{1}{\sqrt{\pi\tau}}\,e^{-(a^2+\lambda)\tau}\right],$$

$$f_{13}(\xi,\lambda,\tau)=\frac{e^{\lambda\tau}}{\lambda}\left[\sqrt{\lambda\xi}\;\mathrm{erf}\left(\sqrt{\lambda\tau}\right)+\frac{1}{\sqrt{\pi\tau}}\,e^{-\lambda\tau}\right]-\frac{1}{\lambda}\sqrt{\frac{\xi}{\pi\tau}}$$